Actin Polymerization and Depolymerization Coupled to Cooperative Hydrolysis –
EPAPS Appendices

Xin Li[1], Jan Kierfeld[2], and Reinhard Lipowsky[1]

[1] *Theory & Bio-Systems, Max Planck Institute of Colloids and Interfaces, 14424 Potsdam, Germany and*
[2] *Physics Department, TU Dortmund University, 44221 Dortmund, Germany* *

(Dated: May 19, 2009)

As in the main text, we denote the three protomer (or subunit) species ATP-actin, ADP/P$_i$-actin, and ADP-actin by T, Θ, and D, respectively.

Rates for cooperative ATP cleavage

For cooperative ATP cleavage of a T protomer, we distinguish the three local neighborhoods TT, TΘ, and TD and the corresponding ATP cleavage rates ω_{cT}, $\omega_{c\Theta}$ and ω_{cD}. In order to eliminate one parameter, we take $\omega_{c\Theta} = \omega_{cD} = \omega_c$ and put $\omega_{cT} = \rho_c \omega_c$, see equation (2) of the main text.

In principle, an alternative choice seems to be $\omega_{cD} = \omega_c$ and $\omega_{cT} = \omega_{c\Theta} = \rho_c \omega_c$. However, if we then considered the limiting case of vectorial cleavage with $\rho_c = 0$, this limiting situation would be inconsistent with the hydrolysis process (VR) as observed experimentally in [1]. This can be understood as follows.

In the vectorial limit with $\omega_{cT} = \omega_{c\Theta} = 0$, the filament would exhibit only two protomer patterns: (i) a single Θ protomer between the T cap and the D core, and (ii) no Θ protomer between the T cap and the D core. The total cleavage flux J_c is then given by $J_c = \omega_c \omega_r/(\omega_c + \omega_r)$ with the P$_i$ release rate ω_r for the Θ protomer at the ΘD domain boundary. This expression implies the asymptotic behavior $J_c \approx \omega_r$ for $\omega_r \ll \omega_c$ which is inconsistent with the process (VR). Indeed, process (VR) is characterized (i) by $\omega_r \ll \omega_c$, see Table 1 in the main text, and (ii) by $J_c = \omega_c$ for actin concentrations $C_T > C_{T,c}$, see Fig. 2 in the main text.

First protomer at barbed end

We now discuss the steady state probabilities $P_T(1)$, $P_\Theta(1)$, and $P_D(1)$ that the first protomer at the barbed end is a T, Θ and D protomer, respectively. The functional dependence of these probabilities on the actin concentration C_T is shown in Fig. 5 for process (RR) consisting of random ATP cleavage followed by random P$_i$ release with $\rho_c = \rho_r = 1$ as defined in Table 1 of the main text.

In the absence of any actin monomers in the surrounding solution, i.e., for $C_T = 0$, one has $P_D(1) = 1$ and $P_T(1) = P_\Theta(1) = 0$ corresponding to a continuously depolymerizing filament that consists only of D protomers. As the concentration C_T is increased, the probability $P_D(1)$ for a D end decreases and the probability $P_T(1)$
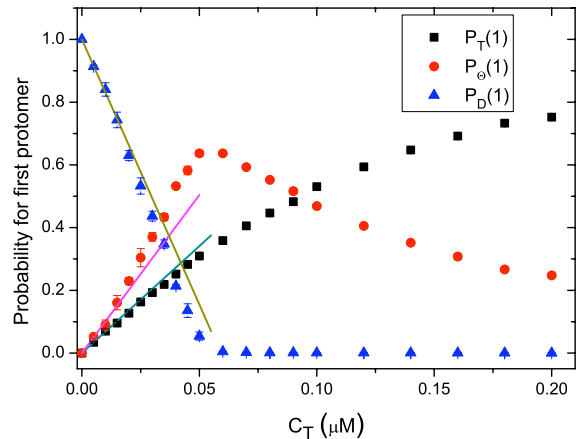

FIG. 5: Steady state probabilities $P_T(1)$, $P_\Theta(1)$, and $P_D(1)$ that the first protomer at the barbed end is a T, Θ, and D protomer, respectively, as functions of actin concentration C_T for the process (RR) as defined in the main text, see Table 1. The three straight lines correspond to the analytical expressions that describe the asymptotic behavior for small C_T.

for a T end increases monotonically whereas the probability $P_\Theta(1)$ for a Θ end increases for small C_T and decreases for large C_T, see Fig. 5. The latter figure also shows that the large concentration regime is characterized by $P_T(1) \approx 1$ and $P_D(1) \approx P_\Theta(1) \approx 0$ as expected. For small C_T, one has $P_T(1) \sim P_\Theta(1) \sim C_T$ and $1 - P_D(1) \sim C_T$. It is not difficult to calculate the corresponding expansion coefficients. As shown in Fig. 5, the resulting expressions are in very good agreement with the simulation data for small concentration C_T.

Flux balance relations for steady states

Next, we express the global fluxes as provided by the filament growth rate J_g, the total ATP cleavage flux J_c, and the total P$_i$ release flux J_r in terms of the three probabilities $P_T(1)$, $P_\Theta(1)$, and $P_D(1)$.

In the steady state, the filament growth (or elongation) rate J_g, which is measured in units of protomers per unit time, has the general form

$$J_g = \omega_{on} - P_T(1)\,\omega_{off,T} - P_\Theta(1)\,\omega_{off,\Theta} - P_D(1)\,\omega_{off,D} \quad (1)$$

with $\omega_{on} = \kappa_{on} C_T$ as defined in the main text. Likewise, the total ATP cleavage flux J_c is given by $J_c = \omega_{on} - P_T(1)\,\omega_{off,T}$ and the total P$_i$ release flux J_r by $J_r = \omega_{on} -$

$P_{\mathrm{T}}(1)\,\omega_{\mathrm{off,T}} - P_{\Theta}(1)\,\omega_{\mathrm{off,\Theta}}$. A combination of these two relations leads to

$$J_{\mathrm{r}} = J_{\mathrm{c}} - P_{\Theta}(1)\,\omega_{\mathrm{off,\Theta}} \qquad (2)$$

between the total P_i release flux J_{r} and the total ATP cleavage flux J_{c}. This relation implies for the three processes (RR), (VR), and (SS) that the two fluxes J_{c} and J_{r} are approximately equal for all actin concentrations C_{T} as shown in Fig. 2 in the main text. Indeed, the difference between these two fluxes is equal to $P_{\Theta}(1)\,\omega_{\mathrm{off,\Theta}}$, which represents a small correction since (i) the probability $P_{\Theta}(1)$ vanishes both for small and for large C_{T}, see Fig. 5, and (ii) the detachment rate $\omega_{\mathrm{off,\Theta}} = 0.2/\mathrm{s}$ for the processes (RR) and (VR) and $\omega_{\mathrm{off,\Theta}} = 0.1/\mathrm{s}$ for the process (SS), see Table 1 in the main text.

Fluxes for small and large concentrations

For large concentrations C_{T}, the three barbed end probabilities behave as $P_{\mathrm{T}}(1) \approx 1$ and $P_{\mathrm{D}}(1) \approx P_{\Theta}(1) \approx 0$, see Fig. 5. When these expressions are inserted into relation (1) for the filament growth rate J_{g}, one obtains the asymptotic behavior

$$J_{\mathrm{g}} \approx \kappa_{\mathrm{on}}\, C_{\mathrm{T}} - \omega_{\mathrm{off,T}} \quad \text{for large} \quad C_{\mathrm{T}}. \qquad (3)$$

Likewise, the behavior of the three probabilities $P_{\mathrm{T}}(1)$, $P_{\Theta}(1)$, and $P_{\mathrm{D}}(1)$ for small C_{T} leads to the asymptotic behavior

$$J_{\mathrm{g}} \approx -\omega_{\mathrm{off,D}} + \frac{\omega_{\mathrm{c}}\phi + \omega_{\mathrm{off,D}}}{\omega_{\mathrm{c}} + \omega_{\mathrm{off,T}}}\,\kappa_{\mathrm{on}}\,C_T \qquad (4)$$

for small C_{T} with $\phi \equiv (\omega_{\mathrm{r}} + \omega_{\mathrm{off,D}})/(\omega_{\mathrm{r}} + \omega_{\mathrm{off,\Theta}})$. The asymptotic behavior as given by (3) and (4) is in very good agreement with the simulation data for J_{g}, see Fig. 6. The same agreement is found for the total cleavage flux J_{c} and the total P_i release flux J_{r}.

Threshold concentration for vectorial ATP cleavage

For vectorial ATP cleavage with cleavage parameter $\rho_{\mathrm{c}} = 0$, a T protomer cannot be cleaved if its nucleotide binding pocket is close to another T protomer. As a consequence, all protomer patterns of the filament have at most one TΘ or one TD domain boundary and the total ATP cleavage flux J_{c} cannot exceed the cleavage rate $\omega_{\mathrm{c}} = \omega_{\mathrm{c\Theta}} = \omega_{\mathrm{cD}}$ at such a domain boundary, i.e., $J_{\mathrm{c}} \le \omega_{\mathrm{c}}$.

For any steady state, the excess number of T protomers added to the filament per unit time is given by

$$J_{+\mathrm{T}} = \omega_{\mathrm{on}} - P_{\mathrm{T}}(1)\,\omega_{\mathrm{off,T}} = \kappa_{\mathrm{on}}\,C_{\mathrm{T}} - P_{\mathrm{T}}(1)\,\omega_{\mathrm{off,T}}. \quad (5)$$

For sufficiently small C_{T}, the T protomer at the barbed end may be cleaved before another T monomer is attached which leads to a temporary protomer pattern with

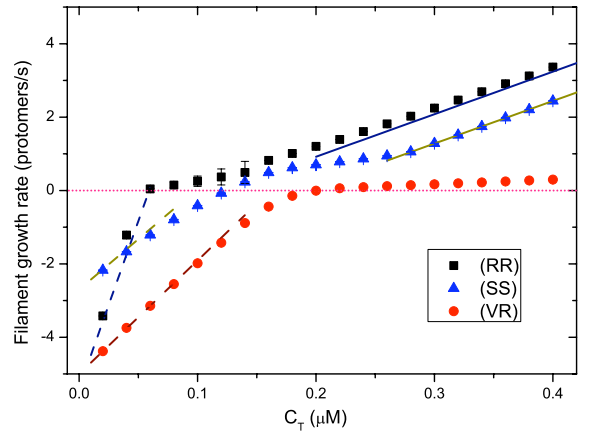FIG. 6: Filament growth rate J_{g} in units of protomers per second as a function of actin concentration C_{T} for the three hydrolysis processes (RR), (VR), and (SS) as defined in the main text, see Table 1. The lines correspond to the asymptotic behavior as given by (3) and (4).

no T protomer and, thus, no TΘ and no TD domain boundary. Since the latter pattern does not contribute to the total cleavage flux J_{c}, one has $J_{\mathrm{c}} < \omega_{\mathrm{c}}$ and a regular steady state with $J_{+\mathrm{T}} = J_{\mathrm{c}}$.

For sufficiently large C_{T}, on the other hand, the incoming excess flux $J_{+\mathrm{T}}$ exceeds the cleavage rate ω_{c} at the TΘ domain boundary and the system attains a singular steady state characterized by a continuously growing T cap and $J_{\mathrm{c}} = \omega_{\mathrm{c}}$. In such a state, the first protomer at the barbed end is always in the T state which implies $P_{\mathrm{T}}(1) = 1$ and $P_{\Theta}(1) = P_{\mathrm{D}}(1) = 0$. The threshold concentration $C_{\mathrm{T,c}}$ between the small and the large concentration regimes is then determined by the two conditions

$$J_{+\mathrm{T}} = \kappa_{\mathrm{on}}\,C_{\mathrm{T,c}} - P_{\mathrm{T}}(1)\,\omega_{\mathrm{off,T}} = \omega_{\mathrm{c}} \qquad (6)$$

and $P_{\mathrm{T}}(1) = 1$ which implies $C_{\mathrm{T,c}} = (\omega_{\mathrm{c}} + \omega_{\mathrm{off,T}})/\kappa_{\mathrm{on}}$, i.e., equation (4) in the main text. The same threshold also follows from a simplified model for vectorial cleavage with only two protomeric species as studied in [1, 2].

Threshold concentration for vectorial P_i release

For vectorial P_i release with $\rho_{\mathrm{r}} = 0$, a Θ protomer cannot release its P_i if the nucleotide binding pocket of this Θ protomer is close to a T or another Θ protomer. As a consequence, all protomer patterns of the filament have at most one ΘD domain boundary and the total P_i release flux cannot exceed the P_i release rate $\omega_{\mathrm{r}} = \omega_{\mathrm{rD}}$ at this boundary, i.e., $J_{\mathrm{r}} \le \omega_{\mathrm{r}}$.

For any steady state, the excess number of Θ protomers added to the filament per unit time is equal to $J_{+\Theta} = J_{\mathrm{c}} - P_{\Theta}(1)\,\omega_{\mathrm{off,\Theta}}$ or

$$J_{+\Theta} = \kappa_{\mathrm{on}}\,C_{\mathrm{T}} - P_{\mathrm{T}}(1)\,\omega_{\mathrm{off,T}} - P_{\Theta}(1)\,\omega_{\mathrm{off,\Theta}}. \quad (7)$$

For sufficiently small C_T, the Θ protomer may detach from the filament before its P_i has been released which leads to a temporary filament pattern with no Θ protomer and, thus, no ΘD domain boundary. Since the latter pattern does not contribute to the total P_i release flux, one has $J_r < \omega_r$ and a regular steady state with $J_{+\Theta} = J_r$.

For sufficiently large C_T, on the other hand, the incoming excess flux $J_{+\Theta}$ exceeds the P release rate ω_r at the ΘD domain boundary and the system attains a singular steady state characterized by a continuously growing T/Θ cap and $J_r = \omega_r$. In such a state, the first protomer at the barbed end is either in the T or in the Θ state which implies $P_T(1) + P_\Theta(1) = 1$ and $P_D(1) = 0$. The second threshold concentration $C_{T,r}$ is then determined by the two conditions

$$J_{+\Theta} = \kappa_{on} C_{T,r} - P_T(1)\,\omega_{off,T} - P_\Theta(1)\,\omega_{off,\Theta} = \omega_r \quad (8)$$

and $P_T(1) + P_\Theta(1) = 1$. These two relations are equivalent to the implicit equation

$$\omega_r = \kappa_{on} C_{T,r} - P_T(1)\,\omega_{off,T} - (1 - P_T(1))\,\omega_{off,\Theta} \quad (9)$$

which is identical with equation (5) of the main text, where the probability $P_T(1)$ is a monotonically increasing function of $C_T = C_{T,r}$, see Fig. 5.

Since $0 \leq P_T(1) \leq 1$, the implicit equation (9) leads to the inequalities

$$\min(C_1, C_2) \leq C_{T,r} \leq \max(C_1, C_2) \quad (10)$$

with $C_1 \equiv (\omega_r + \omega_{off,T})/\kappa_{on}$ and $C_2 \equiv (\omega_r + \omega_{off,\Theta})/\kappa_{on}$. For $\omega_{off,\Theta} = \omega_{off,T}$, one obtains the explicit solution $C_{T,r} = (\omega_r + \omega_{off,T})/\kappa_{on}$ for all values of ρ_c.

Protomer density profiles

The behavior of the three protomer densities $P_T(x)$, $P_\Theta(x)$, and $P_D(x)$ is displayed in Fig. 7 for the three processes (RR), (VR), and (SS) at two different actin concentrations, $C_T = 0.3~\mu M$ and $6~\mu M$. Inspection of this figure reveals that all three processes (RR), (VR), and (SS) lead to filaments with three distinct segments: a T cap, an intermediate Θ segment, and a D core. Even though these distinct filament segments are always present, their size is very different for the different processes.

For process (VR) and actin concentration $C_T = 0.3~\mu M$, for example, the probability $P_T(1) \simeq 0.03 \ll 1$ and the T cap is much shorter than a single protomer, see Fig. 7(b). Another extreme case is found for process (SS) and actin concentration $C_T = 6~\mu M$, see Fig. 7(f), with a T cap that consists of about 5×10^4 protomers. Long actin filaments in solution have a typical length of 15 - 20 μm corresponding to 5000 - 7000 protomers. Thus, from an experimental point of view, one can reach the steady state for the processes in Fig. 7(a)–(c) and (e) but not for the processes (RR) and (SS) at concentration $C_T = 6~\mu M$ as displayed in Fig. 7(d) and (f).

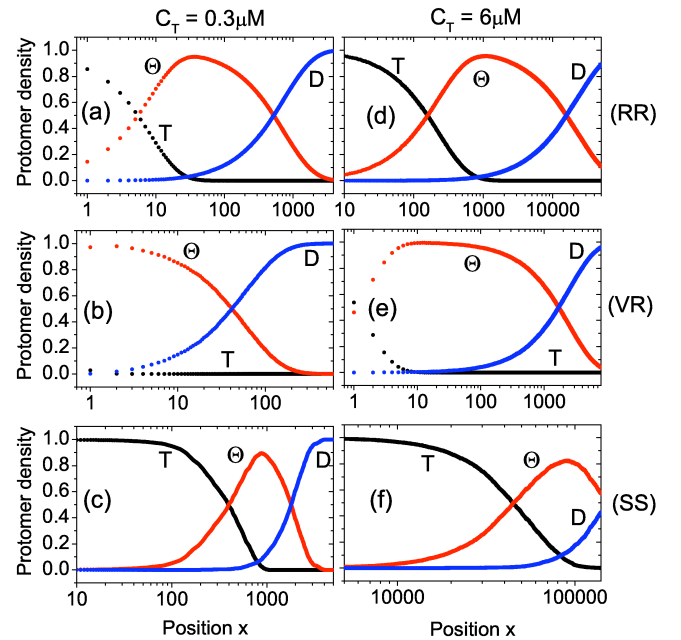FIG. 7: Densities P_α for $\alpha = T$, Θ, and D protomers as a function of the protomer position x. The first protomer at the barbed end is located at $x = 1$ with $P_\alpha(1)$ as in Fig. 5. The densities in the left column (a-c) are obtained for actin concentration $C_T = 0.3~\mu M$, those in the right column (d-f) for $C_T = 6~\mu M$. The first, second, and third row correspond to the three processes (RR), (VR), and (SS) with transition rates as in Table 1. The position x is measured in units of the projected protomer length equal to 2.75 nm.

Strongly cooperative ATP cleavage

As long as the cleavage parameter $\rho_c > 0$, the filament attains a regular steady state with a stationary protomer pattern. For such a state, we may decompose the average number $\langle N_T \rangle$ of T protomers according to

$$\langle N_T \rangle = \langle N_{TT} \rangle + \langle N_{T\Theta} \rangle + \langle N_{TD} \rangle \quad (11)$$

where $\langle N_{TT} \rangle$, $\langle N_{T\Theta} \rangle$, and $\langle N_{TD} \rangle$ denote the average numbers of T protomers that have a T, Θ, and D protomer close to their nucleotide binding pocket, respectively. It is useful to note that $\langle N_{T\Theta} \rangle$ represents the number of $T\Theta$ domain boundaries while $\langle N_{TD} \rangle$ counts the number of TD domain boundaries. Away from the barbed end, a TD domain boundary can only be created by the destruction of a $T\Theta$ domain boundary, a process that does not change the combined number $\langle N_{TX} \rangle \equiv \langle N_{T\Theta} \rangle + \langle N_{TD} \rangle$ of $T\Theta$ and TD domain boundaries.

Using these mutually exclusive subsets of T protomers, we can also decompose the total ATP cleavage flux as

$$J_c = \langle N_{TT} \rangle \rho_c\,\omega_c + \langle N_{TX} \rangle \omega_c \quad (12)$$

where the first term on the right hand side represents the rate at which new $T\Theta$ domain boundaries are being cre-

ated. The latter process increases the combined number $\langle N_{\text{TX}} \rangle$ of TΘ and TD domain boundaries.

For a regular steady state, the flux balance relations imply that the total ATP cleavage rate J_c is equal to the incoming excess flux J_{+T}, i.e., $J_c = J_{+T} = \kappa_{\text{on}} C_T - P_T(1) \omega_{\text{off,T}}$. If this equation is combined with the decomposition (12) of the total cleavage flux J_c, one obtains the flux balance relation

$$\langle N_{\text{TT}} \rangle \rho_c \omega_c + \langle N_{\text{TX}} \rangle \omega_c = J_{+T} . \tag{13}$$

In the limit of small ρ_c, the filament develops a diverging T cap, which implies $\langle N_{\text{TT}} \rangle \gg \langle N_{\text{TX}} \rangle$ and $\langle N_T \rangle \approx \langle N_{\text{TT}} \rangle$. It is now convenient to define the density

$$n_{\text{TX}} \equiv \frac{\langle N_{\text{TX}} \rangle}{\langle N_T \rangle} = \frac{\langle N_{\text{TΘ}} \rangle + \langle N_{\text{TD}} \rangle}{\langle N_T \rangle} \tag{14}$$

of the TΘ and TD domain boundaries which behaves as $n_{\text{TX}} \approx \langle N_{\text{TX}} \rangle / \langle N_{\text{TT}} \rangle$ for small ρ_c. Using this latter equation, the flux balance relation (13) can be rewritten as

$$n_{\text{TX}} \approx \frac{J_{+T}}{\langle N_{\text{TT}} \rangle \omega_c} - \rho_c \tag{15}$$

which shows explicitly that the density n_{TX} of the domain boundaries vanishes as $1/\langle N_{\text{TT}} \rangle$ for small ρ_c.

We now use a scaling argument in order to obtain a second relation between the density n_{TX} and the protomer number $\langle N_{\text{TT}} \rangle$ in the limit of small ρ_c. During a time interval Δt, filament growth leads to the addition of $\Delta t \, J_{+T}$ new T protomers which form a continuous T cap until this cap is broken up by the cleavage of one T protomer and, thus, by the creation of an additional TΘ domain boundary. The scaling argument now consists of the assumption that the resulting density of TΘ (and TD) domain boundaries close to the barbed end is proportional to the overall density n_{TX}. It then takes the time $\Delta t_1 \sim 1/n_{\text{TX}} J_{+T}$ until the continuous T cap at the barbed end breaks up by the creation of an additional TΘ domain boundary. On the other hand, the subset of all T protomers with a TT neighborhood creates new TΘ domain boundaries with the rate $\langle N_{\text{TT}} \rangle \rho_c \omega_c$. Selfconsistency now implies the condition $\Delta t_1 \langle N_{\text{TT}} \rangle \rho_c \omega_c \sim 1$ or $\langle N_{\text{TT}} \rangle \rho_c \omega_c = c_T \, n_{\text{TX}} J_{+T}$ with a dimensionless proportionality coefficient c_T. If this selfconsistency condition is combined with relation (15), one obtains

$$\langle N_{\text{TT}} \rangle \approx b_T \, J_{+T} / \omega_c \sqrt{\rho_c} \tag{16}$$

for small ρ_c with $b_T \equiv \sqrt{c_T}$. This relation is equivalent to equation (7) in the main text since $\langle N_T \rangle \approx \langle N_{\text{TT}} \rangle$ for small ρ_c and $J_{+T} \approx \kappa_{\text{on}} C_T - \omega_{\text{off,T}}$ for large C_T with $P_T(1) \approx 1$.

It then follows that the average number $\langle N_T \rangle$ of T protomers is dominated by the T protomers within the T cap, which contribute the term $\langle N_{\text{TT}} \rangle \sim 1/\sqrt{\rho_c}$ in the decomposition (11) of $\langle N_T \rangle$, whereas the total cleavage flux J_c is dominated by the cleavage at the TΘ domain boundaries, which contribute the term proportional to $\langle N_{\text{TX}} \rangle \sim \mathcal{O}(1)$ in the decomposition (12) of J_c.

The scaling argument just described can be confirmed in a systematic way by calculating the size distribution of T domains for a simplified model in which the two protomeric species Θ and D are combined into a single species. This computation, which will be described elsewhere [3], leads to the value $b_T = \sqrt{\pi/2}$ for the dimensionless coefficient, in very good agreement with the stochastic simulations.

Average number of Θ protomers

For *random* P_i release after *random* cleavage, the average number $\langle N_\Theta \rangle$ of Θ protomers behaves as

$$\langle N_\Theta \rangle \approx \langle N_T \rangle \, \omega_c / \omega_r \tag{17}$$

for large actin concentrations. The transition rates in Table 1 imply $\langle N_\Theta \rangle \approx 100 \langle N_T \rangle$ for process (RR).

For *random* P_i release after *vectorial* cleavage, the average number of Θ monomers has the steady state value

$$\langle N_\Theta \rangle = \omega_c / \omega_r \quad \text{for} \quad C_T > C_{T,c} . \tag{18}$$

The transition rates in Table 1 lead to $\langle N_\Theta \rangle = 4.5 \times 10^3$ for process (VR) with $C_T > 11.0 \, \mu\text{M}$.

Finally, for *strongly cooperative* P_i release after *strongly cooperative* ATP cleavage, a detailed analysis shows that

$$\langle N_\Theta \rangle \approx \langle N_T \rangle \, \frac{\omega_c \sqrt{\rho_c}}{\omega_r \sqrt{\rho_r}} = \langle N_T \rangle \, \frac{\sqrt{\omega_{cD} \, \omega_{cT}}}{\sqrt{\omega_{rD} \, \omega_{r\Theta}}} \tag{19}$$

for $C_T > C_{T,r}$. The transition rates in Table 1 imply $\langle N_\Theta \rangle \approx 2.15 \langle N_T \rangle$ for process (SS).

The asymptotic relations as given by (17) – (19) have been included in Fig. 3(b) and agree very well with the results of the stochastic simulations.

---

* www.mpikg.mpg.de/theory/
[1] M.-F. Carlier, D. Pantaloni, and E.D. Korn. J. Biol. Chem. **262**, 3052 (1987).
[2] E.B. Stukalin and A. Kolomeisky. Biophys. J. **90**, 2673 (2006).
[3] X. Li, R. Lipowsky, and J. Kierfeld. (in preparation).